Design and Evaluation of a Knee Flexion Assistance Exoskeleton for People with Transtibial Amputation

Anthony J. Anderson, Yuri F. Hudak, Kira A. Gauthier, Brittney C. Muir, and Patrick M. Aubin

Abstract— **People with below-knee amputation walk with asymmetric gaits that over time can lead to further musculoskeletal disorders and decreased quality of life. While prosthesis technology is improving, prosthetic ankles may be fundamentally limited in their ability to restore healthy walking patterns because they do not assist the residual knee joint. The knee on the residual limb has muscular deficits due to the loss of the gastrocnemius, a biarticular muscle that crosses both the ankle and knee. Here we present the design, development, and preliminary evaluation of a robotic knee exoskeleton for people with transtibial amputation. The device is intended to restore gastrocnemius-like flexion moments to the knee on the residual limb. The exoskeleton uses a custom offboard actuation and control system to allow for a simple and lightweight design with high torque capabilities. A preliminary walking experiment with one person with transtibial amputation was conducted. The exoskeleton provided a range of knee flexion torque profiles and had an RMS tracking error of 1.9 Nm across four assistance conditions. This device will be used in future studies to explore the effects of providing knee flexion assistance to people with transtibial amputation during walking. Long term, findings from studies with this exoskeleton could motivate future assistive device designs that improve walking mechanics and quality of life for people with limb loss.**

I. INTRODUCTION

Lower limb amputation is a growing problem in the United States, largely due to increases in vascular diseases like diabetes and peripheral artery disease [1]. People with transtibial amputation exhibit slower walking speeds [2], increased metabolic energy expenditure during walking [3], and asymmetric walking patterns [4] relative to the general population. Over time, cumulative loading asymmetries lead to high levels of musculoskeletal comorbidities like knee osteoarthritis in the sound limb and chronic lower back pain [5]. Novel robotic ankle-foot prostheses promise to improve walking mechanics, but initial clinical outcomes are mixed [6], [7].

Over the last two decades, there has been a large research and development focus on improving prosthetic ankle technology [8]. However, transtibial amputees may also benefit from devices that assist other joints during walking. The residual knee joint exhibits muscular deficits due to the transection of the gastrocnemius muscle during amputation. The gastrocnemius is a large calf muscle that originates on the femur and inserts at the calcaneus via the Achilles tendon and produces coupled ankle plantarflexion and knee flexion moments. This function is not present in people with transtibial amputation, and the consequences of this impairment for walking are largely unknown. It is possible that the benefits of the gastrocnemius at the residual knee joint could be restored to people with transtibial amputation with an assistive knee exoskeleton.

Simulation studies have found that clinically standard energy-storage-and-return prostheses provide the vertical bodyweight support of the soleus muscle during walking, but not the forward propulsion provided by the healthy gastrocnemius [9], [10]. Other simulation and experimental evidence has shown that the gastrocnemius and soleus have synergistic but distinct roles during walking in healthy populations [11]. Powered prosthetic ankles address some of the limitations with passive ankles, e.g., powered push-off, but they actuate the ankle joint only and are therefore fundamentally limited to emulating the behavior of the soleus.

During push-off, plantarflexor moments can induce knee extension through intersegmental dynamics, while knee flexion moments can stabilize the joint and prevent hyperextension [12]. In transtibial amputees, knee flexion moments during push-off are reduced [4], and must be provided entirely by muscles in the hamstrings rather than the gastrocnemius. Many of the muscles in the hamstrings are biarticular at the knee and hip, e.g., the biceps femoris. If biarticular muscles in the hamstrings are used to provide compensatory knee flexion moments, they may create maladaptive hip moments and contribute to asymmetric gait. An exoskeleton that provides knee flexion assistance during push-off may allow for a healthier gait that leads to fewer musculoskeletal comorbidities over time.

Several research groups have investigated the effects of pairing knee flexion assistance with prosthetic ankles. Previously, we built and tested a clutched spring biarticular prosthesis to replicate gastrocnemius function [13]. Other research groups have paired active robotic knee exoskeletons with robotic ankles [14], [15]. Initial results have been mixed, with some participants showing large increases in metabolic walking economy [14]. Further research is needed to understand optimal assistance strategies for an artificial gastrocnemius.

This work introduces the design, development, and preliminary evaluation of a robotic knee flexion exoskeleton for people with transtibial amputation. The device is lightweight and can produce high torques with a custom offboard actuation and control system. The exoskeleton can be used with

*This work was supported by VA RR&D Grants A9243C, RX002357, & RX002130.

A. J. Anderson, Y. F. Hudak, K. A. Gauthier, and B. C. Muir are with the Department of Mechanical Engineering at University of Washington, Seattle, WA, and the Center for Limb Loss and Mobility at the VA Puget Sound Health Care System, Seattle, WA. P.M. Aubin is with the Departments of Mechanical Engineering and Orthopaedic and Sports Medicine at University of Washington, Seattle, WA. (email: ajanders@uw.edu)

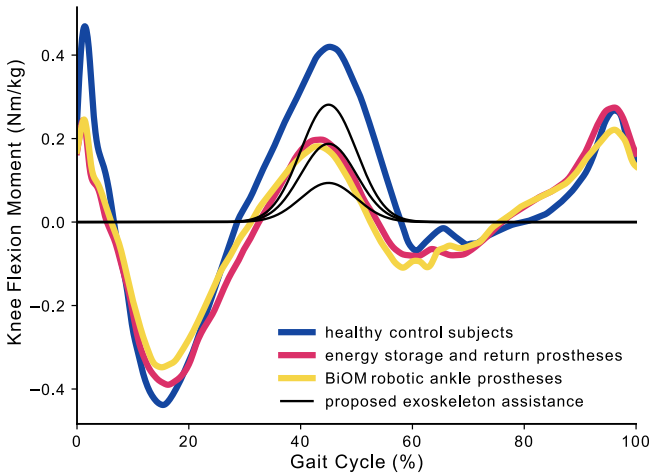

Fig. 1. Knee flexion moments for healthy control subjects and people with limb loss walking on passive and powered prosthetic ankles, digitized from [4]. Flexion moments are notably lower on the residual limb as compared to those from the control subjects, regardless of whether the prosthesis is active or passive. Proposed knee flexion exoskeleton assistance strategies are overlaid in black.

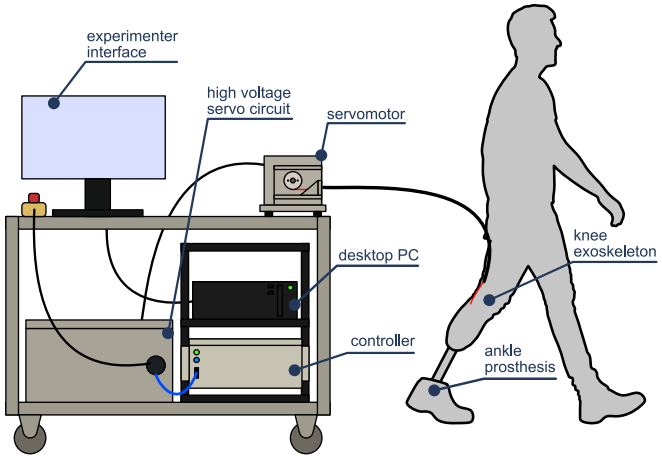

Fig. 2. Schematic of the experimental setup. The participant walks on a treadmill as a stationary motor delivers torque to the knee exoskeleton through a flexible Bowden cable tether. The cart also contains a high-speed computer for taking sensor measurements and sending motor commands. The experimenter interface is a desktop PC that streams data to and from the controller.

either a passive or powered prosthesis. The purpose of this study was to evaluate the mechatronic performance of the exoskeleton while it assisted a participant with transtibial amputation during walking. Our experimental results indicate that the device can successfully provide a variety of knee flexion torque profiles during walking with low torque-tracking error. The exoskeleton described here will be used in future experiments to determine how knee flexion assistance may benefit people with transtibial amputation.

II. MECHATRONIC DESIGN AND CONTROL

The purpose of the exoskeleton is to provide knee flexion moments to the wearer during walking (Fig. 1). Our design intent was to build a lightweight device capable of delivering large moments and forces to the leg. We were inspired by other exoskeletons that achieved these aims with offboard actuation and planar carbon fiber componentry [16], [17]. We made several design decisions that were specific to our intended population of transtibial amputees. For example, we required of our design that the posterior side of the leg was unobstructed when wearing the device so that our subjects could sit in a chair and rest during breaks in the data collection procedure. Additionally, the interface between the exoskeleton and the shank accounted for the prosthetic socket and pylon. We designed and built an offboard actuation system and prototype exoskeleton with a Bowden cable actuated pulley on the lateral side of the knee.

A. Offboard Actuation and Control System

The knee exoskeleton is actuated and controlled by a custom offboard actuation system, which is shown schematically in Fig. 2. The offboard system is called the Configurable Off-Board Robotic Actuator, or COBRA. The primary components of COBRA are 1) a powerful servomotor and flexible transmission tether, 2) a high-speed measurement and control system, and 3) a desktop PC that runs an experimenter interface. These components sit on a cart that is positioned behind an instrumented treadmill during experiments.

The primary actuator for COBRA consists of a 5.47 kW three-phase servomotor (Kollmorgen, AKM74L), an industrial servo drive (Kollmorgen, AKD-P02406), and a custom transmission to transfer motor torque to Bowden cable force. The transmission uses a shaft supported by bearings and pulley to pull on the inner rope of the Bowden cable. The outer Bowden cable sheath is fixed rigidly to the motor chassis. The actuators and open design parameters of COBRA were chosen based on a modeling and optimization framework to minimize the reflected inertia of the system [18].

A high-speed real-time controller (NI, PXIe-8880) measures signals from sensors on the wearable device, computes controller outputs, and sends digital motor commands to the servo drive through an etherCAT connection. The controller communicates with a desktop PC that allows the researcher to change the device behavior, observe sensor measurements from the knee exoskeleton, and log experimental data.

B. Knee Exoskeleton Prototype

The exoskeleton frame is made of a thigh section and a shank section, each of which is composed of flat carbon fiber struts on the medial and lateral sides of the leg (Fig. 3). For both sections, the medial and lateral struts are rigidly connected to each other through a hollow carbon fiber crossbar on the anterior side of the leg. The thigh and calf sections are connected through simple rotary joints on both sides of the knee that are comprised of ball bearings and machined 7075 aluminum components. Thin strips of foam padding line the inside faces of the carbon fiber struts for comfort and to prevent scuffing on the user's prosthetic socket.

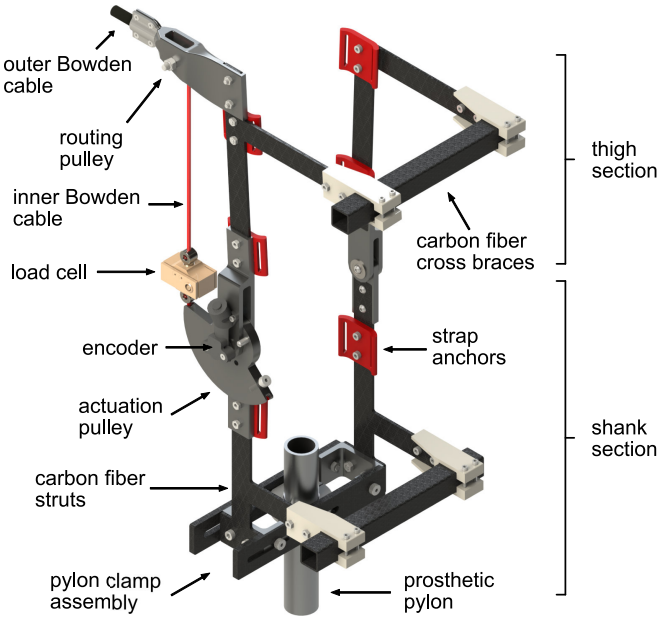

Fig. 3. Rendering of the knee exoskeleton with labels for the primary components described in the text.

The exoskeleton frame delivers forces to the thigh through two sets of straps that weave through thin sheets of foam-backed plastic to distribute load. The straps are simple strips of 1" wide hook-and-loop and connect to the carbon fiber struts through 3D-printed anchor points. The frame connects to the shank section with a similar strap directly below the knee joint that is tightened against the prosthetic socket. Instead of a strap at the distal portion of the shank, the exoskeleton is fixed directly to the prosthetic pylon with carbon fiber crossbars and a 30 mm shaft collar clamp.

The Bowden cable actuator enters the exoskeleton from the posterior direction and is clamped to the lateral carbon fiber strut on the thigh. A pulley routes the inner cable down the side of the thigh to an anchor point on the shank section of the device. The anchor point is built into the lateral section of the rotary joint and constrains the rope to wrap around a constant 0.055 m radius that is machined into the joint structure. We chose to route only the inner cable down the thigh to keep the outer Bowden cable sheath as straight as possible between the motor and the device. Bowden cable friction increases greatly with the total bend angle of the cable, and high levels of friction can degrade controller and actuator performance.

An encoder (RLS, RM08A) on the lateral knee joint measures exoskeleton rotation, and a load cell attached in line with the Bowden cable (Futek, LRF350) measures tension in the rope at the anchor point. The exoskeleton has hard-stops at 5 degrees of hyperextension and 90 degrees of flexion, allowing for a total range of motion of 95 degrees. A smaller rope selected specifically for its tensile strength couples the Bowden cable to the load cell and acts as a safety breakaway to prevent excessively high cable forces.

The exoskeleton fits a variety of leg sizes, as we have multiple distinct sizing options and adjustability within each size. We accommodate different leg lengths by swapping different lengths of carbon fiber struts and can adjust for leg diameter by increasing the length of the carbon fiber cross bars. Mass optimization was a focus of the design, as adding mass to the lower limbs of prosthesis users can reduce their metabolic walking economy [19]. Table I shows a breakdown of the exoskeleton mass.

TABLE I
MASS DISTRIBUTION OF WEARABLE EXOSKELETON COMPONENTS

Component	Mass (g)	(%)
Structural Carbon Fiber	354	25
Metal Joints	152	11
Bowden Cable Inlet & Pulley	218	16
Sensors & Mounts	151	11
Straps & Strap Anchors	216	16
Pylon Clamp Assembly	143	10
Fasteners	160	11
Total:	1394	100

C. Torque Control System

The knee exoskeleton operates in joint torque control mode. The primary functions of the control system are to detect heel strikes, estimate gait phase, compute torque setpoints, and send motor velocity commands. All controller functionality described here was implemented in a custom NI LabVIEW 2018 program.

Vertical ground reaction forces measured by an instrumented treadmill are used to detect heel strikes in real-time. The ground reaction force signal is smoothed with a digital Butterworth filter, and the force rate of change is computed with a finite difference derivative. When the force rate of change exceeds a preset threshold and the magnitude of the ground reaction force is below a separate threshold, heel-strike is identified. Heel-strike data is used to estimate gait phase. In this context, gait phase is defined as the time since the most recent heel strike, normalized by the average stride period over the previous five strides. The exoskeleton uses gait phase as a real-time domain for torque setpoint signals.

The desired knee flexion moment profile is defined using the equation for a Gaussian curve, similar to methods in [20]. The following equation is used to generate the torque setpoint in real-time:

$$\tau = a \cdot \exp(-(\phi - b)^2/2c^2) \quad (1)$$

In (1), τ is the torque setpoint and ϕ is the real-time phase estimate. Parameters a, b, and c scale the peak, midpoint, and width of the Gaussian curve, respectively. These parameters can be changed by the experimenter to explore various knee flexion moment profile shapes during walking. Fig. 1 shows the effect of increasing a while keeping b and c constant.

The tracking controller uses a cascaded control architecture to minimize error between the torque setpoint and the applied exoskeleton torque. An outer torque control loop computes motor velocity setpoint commands that are sent to an inner high-bandwidth motor velocity tracking

loop implemented on the industrial servo-drive. This method has been shown to be successful in Bowden cable driven exoskeletons [17]. The torque tracking loop uses a combination of feedback and feedforward control. For feedback, the controller uses a proportional term on measured torque error and a damping injection term on measured motor velocity. The feedforward controller uses iterative learning methods to overcome systematic tracking error due to the nonlinear effects of Bowden cable friction. Specifically, the torque tracking controller is an implementation of the "PD+LRN" algorithm described in detail in [21]. The command sent to the servo-drive at each loop iteration is defined as:

$$\omega_c = K_p \cdot e_\tau - K_d \cdot \omega_m + \omega_{L,n}(\phi - D) \tag{2}$$

In (2), ω_c is the reference velocity command sent to the servo-drive. K_p and K_d are positive scalar controller gains, and e_τ is the instantaneous torque error. Torque error is the difference between the setpoint torque and the torque estimated from the load cell and known exoskeleton geometry. ω_m is the motor velocity as measured by a digital encoder. $\omega_{L,n}$ is the iteratively learned feedforward motor velocity signal for the current stride, n, gait phase, and a parameter, D, that shifts the signal in time to account for dynamic delays between changes in motor velocity and changes in applied torque. The feedforward signal is updated at each heel strike with the following equation:

$$\omega_{L,n}(\phi) = K_L \cdot e_{\tau,n-1}(\phi) + \beta \cdot \omega_{L,n-1}(\phi) \tag{3}$$

In (3), K_L is a learning gain that scales error from the previous stride and β is a "forgetting" term that is less than one and is used to prevent divergence of the signal. The effect of (3) is that the torque errors and the feedforward signal from the previous stride are scaled and combined to produce the feedforward signal for the current stride.

III. Experimental Methods

The mechanical and control system performance of the knee exoskeleton were evaluated with one subject with transtibial amputation in an IRB-approved research study at the Center for Limb Loss and Mobility within the Veterans Affairs Puget Sound Health Care System. The purpose of this experiment was to perform an initial evaluation of the prototype during walking. The participant was a traumatic unilateral transtibial amputee with no other neurological or orthopedic comorbidities that prevented them from walking.

After an informed-consent process, a certified prosthetist fit the participant with a new ankle prosthesis (Ossur, LP Variflex Foot). This was done because the participant's prosthesis had a built-in torsional adapter that would have interfered with the exoskeleton's pylon attachment. After fitting, the participant was given five minutes to walk at a self-selected pace and adapt to the new ankle. The participant's body mass, leg length (distance from greater trochanter to floor), and height were then recorded as 82.1 kg, 0.87 m, and 1.65 m, respectively. The prosthetist then fit the exoskeleton to the participant. During the fitting process, the prosthetist aligned the rotation axes of the exoskeleton and the knee as closely as possible. Between fit adjustments, the participant flexed and extended their knee and reported on comfort and perceived shear forces at the strap interfaces. The combined mass of the participant and exoskeleton was recorded as 83.6 kg.

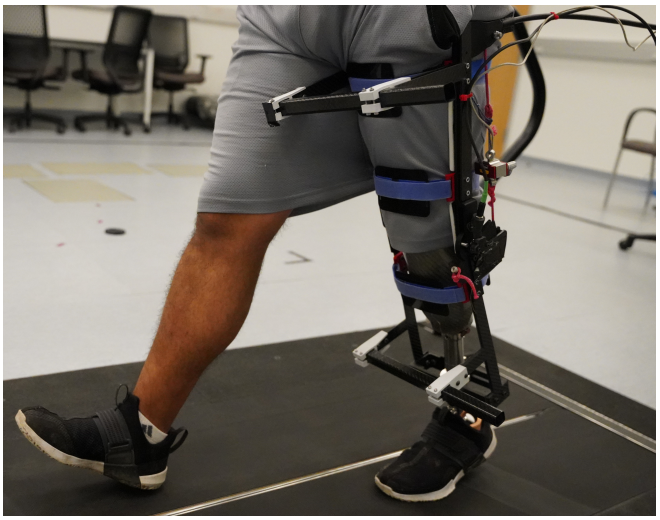

Fig. 4. Photo of the participant walking with the robotic exoskeleton.

For all walking trials, the participant walked on an instrumented treadmill at a non-dimensionalized Froude (Fr) speed of 0.16, where $Fr = v^2/gl$, v is walking speed, l is the measured leg length, and g is the gravitational constant of 9.81 m/s^2. A Fr speed of 0.16 was selected as it is close to self-selected walking speed for people without amputation and allowed us to choose exoskeleton torque magnitudes based on values from the literature [4]. For this participant, the nondimensionalized walking speed corresponded with a treadmill speed of 1.17 m/s.

First, the participant walked on the treadmill for several minutes with the exoskeleton set to 'transparent' mode, meaning only a constant small torque setpoint was commanded to prevent excessive cable slack. Ground reaction force data was collected and visualized to set the initial timing parameters for the exoskeleton assistance. Initial parameters were set such that the peak of the assistance profile occurred at 45% of the gait cycle, turned off completely before swing phase, and had a magnitude of 10 Nm. The participant then walked with the exoskeleton providing a knee flexion moment with these settings for three minutes. At the end of three minutes, the participant was allowed to request changes to the exoskeleton assistance timing parameters (b and c from (1)) to be more comfortable. Parameter selection was achieved through a conversational tuning process between the experimenter, participant, and prosthetist. Once the timing parameters were established, they were held constant throughout the rest of the experiment.

A parameter sweep of the assistance magnitude, a, was performed. The tested magnitudes included 0 Nm/kg through 0.375 Nm/kg in 0.09375 Nm/kg increments, resulting in five

total conditions. Body mass while wearing the exoskeleton was used to scale the assistance magnitude. This range was selected as 0.375 Nm/kg is near the peak knee flexion moment for healthy controls walking at a similar speed (Fig. 1). The participant walked at each setting for roughly three minutes, and two 10-second data collections occurred at each setting. Fig. 4 shows the participant walking in the exoskeleton.

During data analysis, torque tracking errors were evaluated for each condition by concatenating the two 10-second data collections and computing the RMSE between torque command and measurement across the entire gait cycle. Gait cycles were then segmented across all conditions using heel-strike data and were normalized in time. Mean and standard deviation torque signals were computed by averaging all normalized strides within each condition. Stance phase peak torque was identified from the average torque signal for each condition. Exoskeleton range of motion was computed using the encoder signal for each stride and averaged within conditions.

IV. Results

The prosthetist successfully fit the exoskeleton to the participant. Slight lateral bending of the struts allowed for the device to conform to the participant's leg geometry. Clamping the device directly to the prosthetic pylon prevented the device from migrating down the leg during walking, which is a common problem for knee braces and exoskeletons. Measurements of the participant with and without the exoskeleton indicated that the device mass was 1.5 kg. This is slightly more than we found through measurements of the device (Table I) due to the added mass of the Bowden cable actuator.

The final timing parameters selected by the participant, b and c, were 0.44 and 0.07, respectively. The participant completed the first four walking conditions but could not coordinate their gait with the exoskeleton at the highest torque setting (31.35 Nm peak), so data was not collected at this setting. The participant was unable to maintain a steady gait and stated that the treadmill speed would need to be increased for them to walk with the highest setting. It is possible that the participant could have learned to walk with the highest setting with additional time or training, or the assistance level may have simply been too high for the controlled walking speed.

The exoskeleton hardware and software performed as expected during the walking experiment. Fig. 5 shows several of the signals measured from the participant and device during a representative 10-second trial. Table II shows how torque tracking error, peak torque, and exoskeleton range of motion vary with assistance magnitude. The peak torque during stance increased with the assistance magnitude setpoint as expected. Variability in exoskeleton range of motion within and across conditions was under 3 degrees, which is 5% of the average range of motion across all trials.

Torque tracking errors were generally low, except for during swing phase. During late swing, the knee extends rapidly to position the foot for the upcoming heel strike.

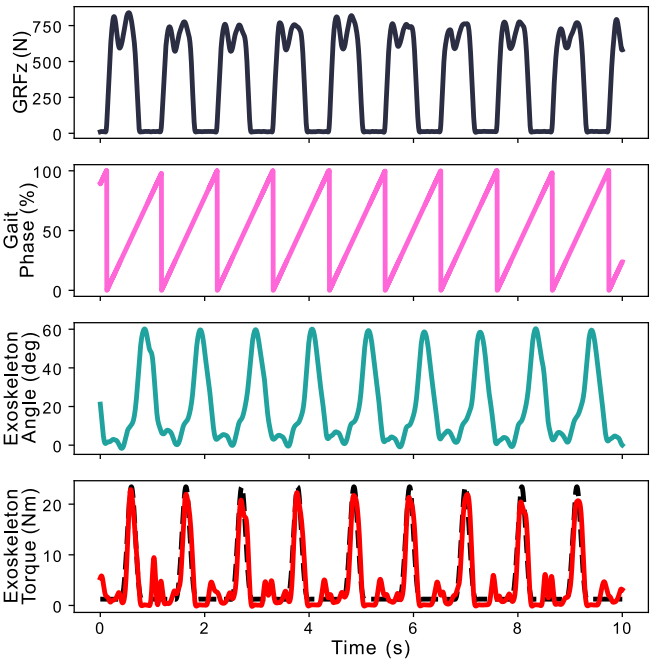

Fig. 5. Plots of relevant real-time controller signals for a representative trial. Vertical ground reaction forces are measured as an analog input from the split-belt instrumented treadmill. Gait phase is estimated in real-time from ground reaction force data. The exoskeleton encoder measures rotation of the biological knee joint and additional rotation due to soft tissue compression during actuation. In the exoskeleton torque plot, the black dashed line is the setpoint and the red line is the measured exoskeleton torque.

TABLE II
Exoskeleton Performance Metrics Across Conditions

Assistance Magnitude, a, (Nm)	RMS Tracking Error (Nm)	Peak Torque (SD) (Nm)	Range of Motion (SD) (deg)
0	1.43	3.02 (0.46)	57.2 (1.4)
7.84	1.67	8.37 (0.34)	56.16 (0.33)
15.68	2.61	16.34 (0.46)	57.87 (0.85)
23.51	1.88	21.44 (0.68)	59.06 (0.95)

At this instant, the motor must unspool the Bowden cable quickly to avoid applying a flexion moment. Though the motor unspools at roughly 800 degrees/second, friction in the cable housing causes some force to develop in the cable. However, we consider this tracking error to be of relatively little concern, as the biological knee also exhibits a knee flexion moment in late swing to decelerate the limb. Fig. 6 shows the tracking performance of the exoskeleton over the average stride for the four conditions.

The participant's feedback on the exoskeleton was generally positive. They stated that the device "made their leg feel more stable" and gave them a "more powerful stride." They also noted that the device altered the way forces were transmitted to their residual limb through the prosthetic socket but had no feedback on whether the change was positive or negative.

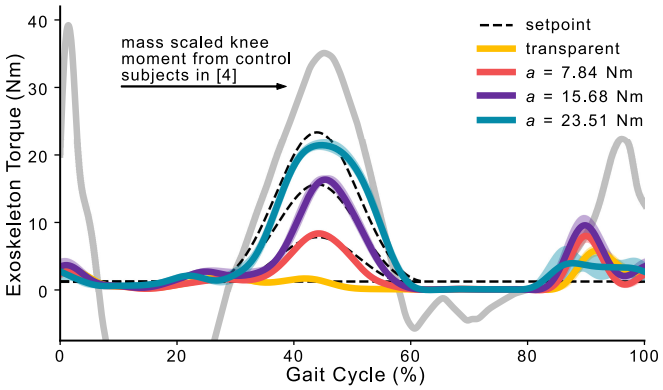

Fig. 6. Applied exoskeleton torques across four assistance magnitudes. Mean strides for each condition ± one standard deviation are shown. The average biological knee moment from control subjects in [4] is overlaid to give context to the timing and magnitude of the exoskeleton torque profiles. Exoskeleton torques are low during early stance and swing for all conditions, indicating that the device can behave transparently when desired.

V. Discussion

In this paper, we presented the design and control of a knee exoskeleton for transtibial amputees and a preliminary experiment with one participant to evaluate the robotic performance of the device. We found that the exoskeleton could systematically vary the assistance magnitude between nearly-transparent and 65% of the peak biological knee flexion moment with low tracking error. For this preliminary system integration work, we evaluated a torque assistance strategy that is low-dimensional and unlikely to be optimal for transtibial amputee gait, but was relatively easy to tune and understand. Future work with this device will focus on the development of a more flexible and robust assistance strategy and clinical experiments with more subjects.

We chose to develop an exoskeleton with offboard actuation and control hardware, which had several major benefits. Our exoskeleton is lightweight and can produce a broad range of torque profiles. If necessary, future design changes can be made to the exoskeleton end-effector independently of the offboard actuation system. This platform will allow us to rapidly iterate and experiment with knee exoskeleton hardware and assistance strategies to improve walking outcomes and set the design specifications for a future untethered exoskeleton that can be worn outside of the lab. We envision an assistive device that integrates mechanically with the prosthetic socket.

It is currently unknown how the loss of gastrocnemius actuation at the knee affects amputee gait mechanics. Though the neuromuscular system is highly redundant, simulation and experimental work has shown that dysfunction in a single muscle can significantly reduce the feasible set of endpoint forces that a limb can produce [22]. Further biomechanical and clinical experiments are needed to help us understand how assistive technology can improve amputee mobility and health, and exoskeleton testbeds like the one described here are valuable tools for this effort.

References

[1] M. Cai et al., "Temporal Trends in Incidence Rates of Lower Extremity Amputation and Associated Risk Factors Among Patients Using Veterans Health Administration Services From 2008 to 2018," *JAMA Netw. Open*, vol. 4, no. 1, pp. e2033953–e2033953, 2021.

[2] H. R. Batten, S. M. McPhail, A. M. Mandrusiak, P. N. Varghese, and S. S. Kuys, "Gait speed as an indicator of prosthetic walking potential following lower limb amputation," *Prosthet. Orthot. Int.*, vol. 43, no. 2, pp. 196–203, 2019.

[3] R. L. Waters and S. Mulroy, "The energy expenditure of normal and pathologic gait," *Gait Posture*, vol. 9, no. 3, pp. 207–231, 1999.

[4] A. E. Ferris, J. M. Aldridge, C. A. Rábago, and J. M. Wilken, "Evaluation of a Powered Ankle-Foot Prosthetic System During Walking," *Arch. Phys. Med. Rehabil.*, vol. 93, no. 11, pp. 1911–1918, 2012.

[5] R. Gailey, "Review of secondary physical conditions associated with lower-limb amputation and long-term prosthesis use," *J. Rehabil. Res. Dev.*, vol. 45, no. 1, pp. 15–30, 2008.

[6] H. M. Herr and A. M. Grabowski, "Bionic ankle-foot prosthesis normalizes walking gait for persons with leg amputation," *Proc. Biol. Sci.*, vol. 279, no. 1728, pp. 457–464, 2012.

[7] E. S. Gardinier, B. M. Kelly, J. Wensman, and D. H. Gates, "A controlled clinical trial of a clinically-tuned powered ankle prosthesis in people with transtibial amputation," *Clin. Rehabil.*, vol. 32, no. 3, pp. 319–329, 2018.

[8] P. Cherelle, G. Mathijssen, Q. Wang, B. Vanderborght, and D. Lefeber, "Advances in Propulsive Bionic Feet and Their Actuation Principles," *Adv. Mech. Eng.*, vol. 6, p. 984046, 2014.

[9] R. J. Zmitrewicz, R. R. Neptune, and K. Sasaki, "Mechanical energetic contributions from individual muscles and elastic prosthetic feet during symmetric unilateral transtibial amputee walking: A theoretical study," *J. Biomech.*, vol. 40, no. 8, pp. 1824–1831, 2007.

[10] A. K. Silverman and R. R. Neptune, "Muscle and prosthesis contributions to amputee walking mechanics: A modeling study," *J. Biomech.*, vol. 45, no. 13, pp. 2271–2278, 2012.

[11] W. H. Clark, R. E. Pimentel, and J. R. Franz, "Imaging and Simulation of Inter-muscular Differences in Triceps Surae Contributions to Forward Propulsion During Walking," *Ann. Biomed. Eng.*, 2020.

[12] F. E. Zajac and M. E. Gordon, "Determining Muscle's Force and Action in Multi-Articular Movement," *Exerc. Sport Sci. Rev.*, vol. 17, no. 1, pp. 187–230, 1989.

[13] A. M. Willson et al., "Evaluation of a quasi-passive biarticular prosthesis to replicate gastrocnemius function in transtibial amputee gait," *J. Biomech.*, vol. 129, p. 110749, 2021.

[14] M. F. Eilenberg, J.-Y. Kuan, and H. Herr, "Development and Evaluation of a Powered Artificial Gastrocnemius for Transtibial Amputee Gait," *J. Robot.*, vol. 20, 2018.

[15] D. M. Ziemnicki, J. M. Caputo, K. A. McDonald, and K. E. Zelik, "Development and Evaluation of a Prosthetic Ankle Emulator with an Artificial Soleus and Gastrocnemius," *J. Med. Devices*, 2021.

[16] K. A. Witte, A. M. Fatschel, and S. H. Collins, "Design of a lightweight, tethered, torque-controlled knee exoskeleton," in *International Conference on Rehabilitation Robotics*, 2017, pp. 1646–1653.

[17] G. M. Bryan, P. W. Franks, S. C. Klein, R. J. Peuchen, and S. H. Collins, "A hip–knee–ankle exoskeleton emulator for studying gait assistance," *Int. J. Robot. Res.*, p. 25. 2021

[18] A. Anderson, C. Richburg, J. Czerniecki, and P. Aubin, "A Model-Based Method for Minimizing Reflected Motor Inertia in Off-board Actuation Systems: Applications in Exoskeleton Design," in *IEEE 16th International Conference on Rehabilitation Robotics*, 2019, pp. 360–367.

[19] S. J. Mattes, P. E. Martin, and T. D. Royer, "Walking symmetry and energy cost in persons with unilateral transtibial amputations: Matching prosthetic and intact limb inertial properties," *Arch. Phys. Med. Rehabil.*, vol. 81, no. 5, pp. 561–568, 2000.

[20] M. K. Ishmael, M. Tran, and T. Lenzi, "ExoProsthetics: Assisting Above-Knee Amputees with a Lightweight Powered Hip Exoskeleton," in *IEEE 16th International Conference on Rehabilitation Robotics*, 2019, pp. 925–930.

[21] J. Zhang, C. C. Cheah, and S. H. Collins, "Experimental comparison of torque control methods on an ankle exoskeleton during human walking," in *IEEE International Conference on Robotics and Automation*, 2015, pp. 5584–5589.

[22] J. J. Kutch and F. J. Valero-Cuevas, "Muscle redundancy does not imply robustness to muscle dysfunction," *J. Biomech.*, vol. 44, no. 7, pp. 1264–1270, 2011.